https://doi.org/10.5194/cp-2023-47
Preprint. Discussion started: 16 June 2023

Climate of the Past Discussions

Climate and ice sheet dynamics in Patagonia during the Last Glacial Maximum

Andrés Castillo-Llarena[1,2,*], Franco Retamal-Ramírez[3,4,5,*], Jorge Bernales[6], Martín Jacques-Coper[4,5,7], and Irina Rogozhina[2,8,9]

[1]MARUM - Center for Marine Environmental Sciences and Faculty of Geosciences, University of Bremen, Bremen, Germany
[2]Department of Geography, Norwegian University of Science and Technology, Trondheim, Norway
[3]Centro de Investigación Gaia Antártica, Universidad de Magallanes, Punta Arenas, Chile
[4]Departamento de Geofísica, Universidad de Concepción, Concepción, Chile
[5]Center for Climate and Resilience Research (CR)2, Universidad de Concepción, Concepción, Chile
[6]Institute for Marine and Atmospheric Research Utrecht, Utrecht University, Utrecht, Netherlands
[7]Center for Oceanographic Research COPAS COASTAL, Universidad de Concepción, Concepción, Chile
[8]Centro de Estudios Avanzados en Zonas Áridas (CEAZA), La Serena, Chile
[9]Departamento de Ciencias de la Tierra, Universidad de Concepción, Concepción, Chile
[*]These authors contributed equally to this work.

Correspondence: Andrés Castillo-Llarena (acastillollarena@marum.de) and Franco Retamal-Ramírez (fretamal@umag.cl)

Abstract. During the Last Glacial Maximum (LGM, ∼ 23,000 to 19,000 years ago), the Patagonian Ice Sheet (PIS) covered the central chain of the Andes between ∼ 38° S to 55° S. Existing paleoclimatic evidence – mostly derived from glacial landforms – suggests that maximum ice sheet expansions in the Southern and Northern Hemispheres were not synchronized. However, large uncertainties still exist in the timing of the onset of regional deglaciation as well as its major drivers. Here we present an ensemble of numerical simulations of the PIS during the LGM. Our aim is to assess the ability of paleoclimate model products to reproduce the range of atmospheric conditions needed to enable the ice sheet growth in concordance with geomorphological and geochronological evidence. The resulting ensemble is then used as a guideline for the evaluation of the PMIP3 and PMIP4 model performance across different sectors of the former PIS. Our analysis suggests a strong dependence of the PIS geometry on near-surface air temperature forcing. All the ensemble members driven by PMIP products are not able to reproduce the reconstructed ice cover in the northern part of Patagonia. In contrast, the modelled PIS tends to expand beyond its constrained boundaries in south-eastern Patagonia. We largely attribute these discrepancies between the model-based ice geometries and geological evidence to the low resolution of paleoclimate models. We conclude that among all tested climate forcings, the PMIP4 climate models INM-CM4-8 and MPI-ESM1-2-LR produce the necessary conditions for ice sheet growth across Patagonia. It should be kept in mind that this analysis is based only on the evaluation of the modelled ice sheet extent because geological constraints on the former ice thickness are still lacking. Nevertheless, our analysis suggests that a realistic PIS geometry at the LGM can be reproduced only if the complex topographic features of the Andes are properly resolved by climate models.

https://doi.org/10.5194/cp-2023-47
Preprint. Discussion started: 16 June 2023

Climate of the Past Discussions
Open Access
EGU

1 Introduction

At present, there are only two ice sheets on Earth. The Antarctic ice Sheet is the largest, with an ice volume of 26.04 $\pm$ 0.4 $\times 10^6$ km^3 that can be translated into a sea-level equivalent (SLE) of 57.0 $\pm$ 0.9 m (Morlighem et al., 2020). The Greenland Ice Sheet contains 2.99 $\pm$ 0.2 $\times 10^6$ km^3 of ice, which is equivalent to a SLE of 7.42 $\pm$ 0.05 m (Morlighem et al., 2017). However, during the last glacial period, especially during the global Last Glacial Maximum (LGM, 23,000 to 19,000 years before present, ka), much of North America was buried under the North American Ice Sheet complex, the Eurasian Ice Sheet complex stretched across most of Northern Europe, and the Patagonian Ice Sheet (PIS) covered the western part of southern South America. Together, these former ice sheets represented a SLE of around 113.9 m (Simms et al., 2019) and, consequently, global sea level dropped to 120-134 m below present between 29 and 21 ka (Lambeck et al., 2014). As such, this period was marked by partly exposed continental shelves, strong winds, dry conditions, and a total greenhouse gas concentration lower than during the Pre-Industrial (PI; Monnin et al., 2001; Bartlein et al., 2011; Kohfeld et al., 2013; Simms et al., 2019). The latter triggered a lowering of the global mean air temperature, with current estimates of the LGM-PI global surface air (negative) temperature anomaly ranging from 3.2 °C to 6.7 °C (Schneider von Deimling et al., 2006; Holden et al., 2010; Annan and Hargreaves, 2013; Tierney et al., 2020; Kageyama et al., 2021).

The PIS was relatively a small ice sheet, comparable in size to the former Celtic Ice Sheet that covered the British Isles during the LGM (Hughes et al., 2016). At present, its former evolution is subject to considerable uncertainties regarding its past extents, volumes, and relative contributions to sea level variations, mainly due to the scarcity of solid geological evidence. Only recently, Davies et al. (2020) succeeded in building a geochronological data set of a reasonable size and robustness, arriving at the conclusion that the PIS reached its maximum extent at $\sim$ 35 ka. This state remained nearly unchanged until 27 ka, which is much earlier than the global timing estimates for LGM. This is a generic estimate because the evidence suggests that the timing of its maximum extent changed with latitude: the northern sector located between of 38° S to 48° S is thought to have reached its largest area between 33 to 28 ka, while its southern counterpart (between 48° S to 56° S) peaked much earlier, at around 47 ka. Based on simplifying assumptions, Davies et al. (2020) estimated a uniform maximum PIS extent of 492,600 km^2 at 35 ka, corresponding to a SLE of around 1.5 m. To date, the most common way to define the LGM is through a globally integrated ice volume, zooming in on the global climate that was closest to equilibrium during the last glacial period. However, this is a limiting assumption: during the last glacial period, many of the then-existing ice sheets seem to have reached their maximum extent at different dates (Hughes et al., 2013), with both the ice masses and the climate broadly in equilibrium. Studies of past climate conditions commonly rely on global climate models validated and calibrated against paleoclimate proxy data (Braconnot et al., 2012; Annan and Hargreaves, 2013; Evans et al., 2013). This combination of models and observations is a fundamental tool for understanding how Earth's climate has responded to changes in external (e.g. orbit, insolation) and internal (e.g. greenhouse gases) conditions on global and regional scales. When coupled to large water reservoirs, such as the ocean and ice sheets, these models can provide important insights into the role of climate-ocean-ice feedbacks (e.g. albedo, freshwater influx) that can have long response times. To better understand the results from these models, the Paleoclimate Modelling Intercomparison Project (PMIP) has focused exclusively on paleoclimate reconstructions, aiming to provide an

https://doi.org/10.5194/cp-2023-47
Preprint. Discussion started: 16 June 2023


Climate of the Past Discussions

effective mechanism for standardising and coordinating paleoclimate modelling experiments among research groups across the globe (Meinshausen et al., 2011). During the different stages of PMIP (1-4), paleo experiments have been performed with prescribed forcings, including orbital parameters, sea level, topography (including ice sheet elevations), and greenhouse gas concentrations (Joussaume and Taylor, 1995; Braconnot et al., 2007; Harrison et al., 2015; Kageyama et al., 2017).

Recently, Yan et al. (2022) modelled the PIS extent during the LGM combining present-day climatology and PMIP outputs to analyse the degree of agreement between their modelled geometries and the PATICE reconstruction. One of the main findings of their study is that most of the uncertainty in the modelled PIS geometry is associated with the PMIP forcing, producing an overestimation of the ice-covered extent over vast regions, while showcasing an underestimation of ice in other areas. These results reflect the inability of PMIP3 model products to provide climate conditions that allow for ice sheet advance in the northernmost sectors of Patagonia during the LGM, even under a somewhat extreme choice of model parameters. In contrast, some of the PMIP4 models seem to present the climate conditions needed to trigger ice sheet inception and growth in this region. However, Yan et al. (2022) did not provide potential reasons for these discrepancies.

In a much earlier study, Hulton et al. (2002) used numerical modelling to show that a drop in present-day temperatures of at least 6 °C and modified wind patterns (decreasing wind intensity at $\sim$ 50° S where the core of the westerlies is concentrated and increasing them in other latitudes) were a prerequisite for PIS inception. This is because present-day precipitation rates are very high in southern Patagonia and very low in northern Patagonia, compared to a more even distribution during the LGM (Kohfeld et al., 2013).

In this study, we use the numerical ice sheet model SICOPOLIS (Greve, 1997; Sato and Greve, 2012) to explore the range of climate conditions that leads to a good match between the modelled PIS and field-derived geometries. Our ice sheet modelling experiments are driven by climate products from phases 3 and 4 of PMIP. Furthermore, we assess the relative performance of LGM climate forcings in different sectors of the former ice sheet against the geochronological reconstruction of Davies et al. (2020). Finally, we investigate potential reasons for their different performance throughout Patagonia.

2 Methods

2.1 Model set-up

Our PIS simulations cover the area between 80° W and 62° W and between 36° S and 58° S (Fig. 1) and are performed using the open source, three-dimensional, thermomechanical polythermal ice sheet model SICOPOLIS (SImulation COde for POLythermal Ice Sheets) version 5.2 (Greve, 1997; Sato and Greve, 2012). Experiments are designed with an 8 km horizontal resolution and 81 vertical grid points, from which 3 are allocated to the temperate ice layer if it exists. In addition, 41 grid points are reserved for the bedrock, where geothermal flux towards the ice sheet bed is prescribed at the bottom of the bedrock layer.

The model combines the shallow-ice approximation (SIA) and shelfy-stream approximation (SStA) in order to reproduce the entire range of ice flowing conditions across an ice sheet (Bernales et al., 2017). The time step for the calculations of ice velocity, topography changes, internal ice temperature, water content, and age of ice is set to 1 year. At the beginning of each

https://doi.org/10.5194/cp-2023-47
Preprint. Discussion started: 16 June 2023

Climate of the Past Discussions
Open Access
EGU

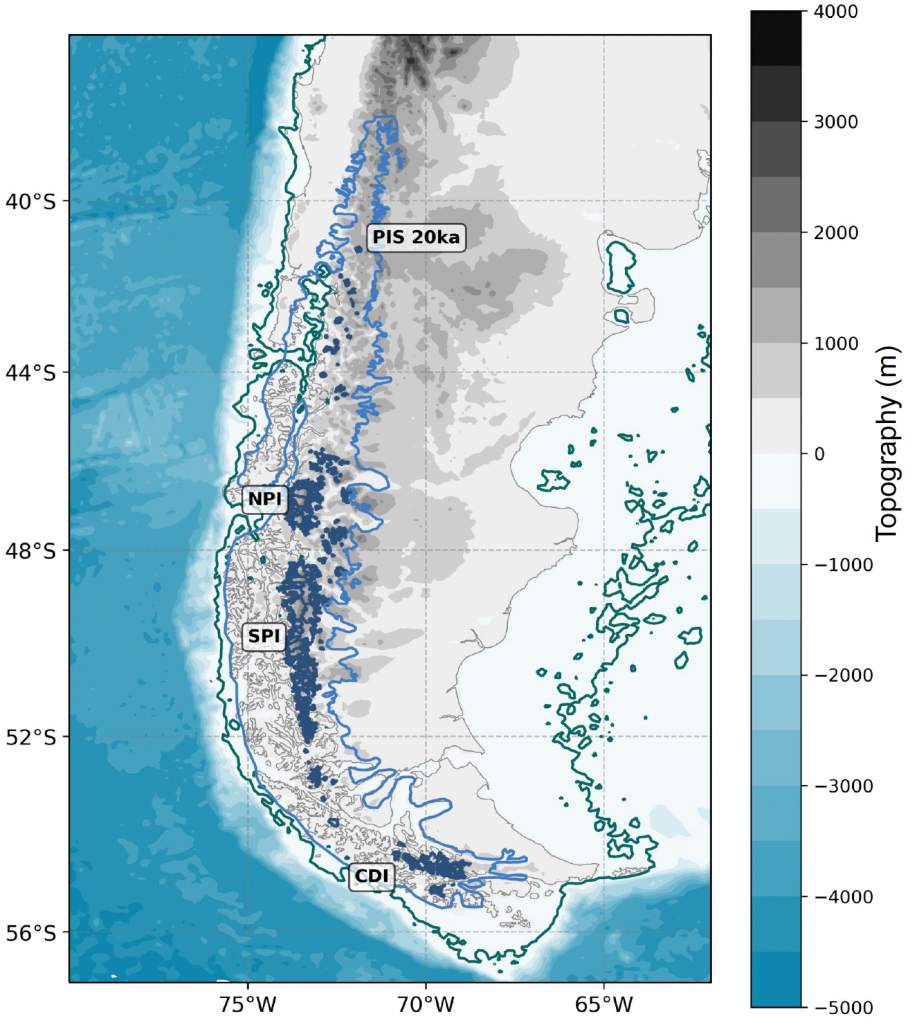

Figure 1. Present-day topographic map of Patagonia based on ETOPO1 (Amante and Eakins, 2009). Present-day ice fields are indicated and correspond to the Northern Patagonian Icefield (NPI), Southern Patagonian Icefield (SPI) and Cordillera Darwin Icefield (CDI). PIS reconstruction of (Davies et al., 2020) for 20 ka. LGM coastal lines marking lower sea level (-120 m) are shown in dark turquoise contour.

https://doi.org/10.5194/cp-2023-47
Preprint. Discussion started: 16 June 2023


Climate of the Past Discussions

simulation, an ice-free topography is prescribed from the ETOPO1 data set (Amante and Eakins, 2009). This initialisation assumes a global sea level drop of 120 m, based on reconstructions for the LGM (Lambeck et al., 2014), which is applied homogeneously over the entire model domain. We use a constant, spatially homogeneous value of 100 $\mathrm{mW\ m^{-2}}$ for the geothermal heat flux, in agreement with averaged values observed in Patagonia (Hamza and Vieira, 2018). Glacial isostatic adjustment is accounted for through an elastic-lithosphere, relaxing-asthenosphere model (ELRA), in which the effects of ice loading and unloading on the planet's surface are parameterised through a constant relaxation time (e.g., Greve and Blatter, 2009).

The surface mass balance is calculated as the difference between ice accumulation and ablation. The latter is computed using a positive-degree-day (PDD) model (Calov and Greve, 2005). Accumulation depends on monthly precipitation and temperature fields, such that the transition between solid and liquid precipitation is linearly proportional to variations in air temperature (Marsiat, 1994). Here we use a transition range of 0 $^{\circ}\mathrm{C}$ to 2 $^{\circ}\mathrm{C}$, producing purely solid or purely liquid precipitation below or above this temperature range, respectively . To account for the discrepancies between the topographies in climate and ice sheet models, near-surface air temperatures are corrected using a lapse rate of -6.5 $\mathrm{K\ km^{-1}}$. At the coasts, where the ice might become afloat, calving at the front of ice shelves is parameterised through an instantaneous calving of ice-filled model cells whose ice thickness becomes thinner than 50 m. General model parameter values used in the ice sheet simulations are summarised in Table 1.

https://doi.org/10.5194/cp-2023-47
Preprint. Discussion started: 16 June 2023


Climate of the Past Discussions

Table 1. Description of the most important parameters in the model set-up.

Model component	Description	Value	Units
Ice rheology			
	Ice density	910.00	$\mathrm{kg\ m^{-3}}$
	Gravity acceleration	9.81	$\mathrm{m\ s^{-2}}$
	Glen's flow law exponent	3.00	-
	Ice specific heat capacity	4170.00	$\mathrm{J\ kg^{-1}\ K^{-1}}$
	Ice thermal conductivity	2.10	$\mathrm{J\ kg^{-1}\ K^{-1}}$
	Water latent heat of fusion	3.34×10^5	$\mathrm{J\ kg^{-1}\ K^{-1}}$
	Enhancement factor for the SIA and SSA	1, 0.5	-
Bedrock			
	Geothermal heat flux	100.00	$\mathrm{W\ m^{-2}}$
	Lithosphere density	3300.00	$\mathrm{kg\ m^{-3}}$
	Sea level	-120.00	m
Surface and atmosphere			
	PDD standard deviation	3	$^\circ\mathrm{C}$
	Temperature of snow precipitation	0	$^\circ\mathrm{C}$
	Temperature of rain precipitation	2	$^\circ\mathrm{C}$
	Degree day factor for snow	8	$\mathrm{mm\ d^{-1}\ ^\circ C^{-1}}$
	Degree day factor for ice	3	$\mathrm{mm\ d^{-1}\ ^\circ C^{-1}}$

2.2 Climate forcing and experimental design

We generate a range of PIS geometries by forcing the ice sheet model with atmospheric products from several climate models that participated in the LGM experiments during phases 3 and 4 of PMIP. Then, we evaluate the resulting geometries against the corresponding time-snapshot at 20 ka from the PATICE geological reconstruction (Davies et al., 2020). Near-surface air temperature and precipitation from thirteen climate models (see Table 2) were used to compute anomalies as the difference (for temperatures) or ratio (for precipitation) between their respective LGM and PI climate snapshots, separately for each climate model. The monthly mean LGM-PI temperature differences are added to the present-day climate from ERA 5, averaged over the period 1979-2020. The monthly mean present-day precipitation fields are multiplied by their corresponding monthly mean LGM/PI precipitation ratios (instead of differences) to prevent negative values. Using the resulting ensemble of precipitation and near-surface temperature pairs as forcing, each ice sheet model simulation is then run for 10,000 model years, which is enough to reach an equilibrium with these time-invariant climate conditions.

https://doi.org/10.5194/cp-2023-47
Preprint. Discussion started: 16 June 2023

Climate of the Past Discussions

Table 2. PMIP3 and PMIP4 models analysed in the present study.

Model name	PMIP phase	Atmospheric model resolution
CCSM4	III	1.25 x 0.9
CNRM-CM5	III	1.4 x 1.4
COSMOS-ASO	III	3.8 x 3.7
FGOALS-g2	III	2.8 x 3-6
GISS-E2-R	III	2.5 x 2.0
IPSL-CM5A-LR	III	3.8 x 1.9
MIROC-ESM	III	2.8 x 2.8
MPI-ESM-P	III	1.88 x 1.9
MRI-CGCM3	III	1.18 x 1.1
INM-CM4	IV	1.5 x 2.0
MPI-ESM1-2-LR	IV	1.88 x 1.88
MIROC-ES2L	IV	2.8 x 2.8
AWI-ESM-1-1-LR	IV	1.88 x 1.88

3 Results

Our model experiments produce a wide range of PIS geometries, some of which are generally comparable with the geologically constrained ice extents, while others yield considerably reduced and/or overextended ice cover (Fig. 2). We have divided the former PIS extent into 3 distinct latitudinal ranges based on their model sensitivity and response to the imposed climate. Each of these areas is described and analysed in detail in the following sections. First, south of 52° S, most ensemble members exhibit an unrealistic build-up of ice in south-eastern Patagonia, with a much larger ice-covered area than inferred from the geological evidence. Second, between 44° S and 52° S, a continuous ice sheet growth is reached by nearly all ensemble members with an overall good match for both eastern and western margins of PATICE. Finally, in the third zone between 38° S and 42° S, PIS growth is not uniformly captured by the ensemble members, with most of them failing to build a consistent ice cover.

Among the PMIP climate model products tested in this study, INM-CM4-8 and MPI-ESM1-2-LR models (both from PMIP4) produce the most consistent ice sheet extents relative to the PATICE reconstruction. The near-surface air temperature and precipitation patterns derived from these two climate models enable the modelled ice sheet to reach as far north as 39° S and 40° S, respectively, and occupy total areas of 519,552 and 423,360 km^2. This is in broad agreement with the earlier estimations by Davies et al. (2020). Total ice volumes produced by these two simulations are 532.4103 and 417.0103 Gt, corresponding to SLEs of 1.47 and 1.15 m (Fig. 2k,l), respectively. In the following, we zoom in on the drivers of the dissimilar model performances across these three distinct zones.

https://doi.org/10.5194/cp-2023-47
Preprint. Discussion started: 16 June 2023


Climate of the Past Discussions

3.1 Excessive Patagonian ice cover in south-eastern Patagonia

Our model experiments show that across southernmost Patagonia (52° S to 56° S), most ensemble members exhibit an unrealistic build-up of ice, with a much larger eastern ice extent than inferred from the geological evidence (Fig. 2). In some cases (e.g., ensemble members driven by CCSM4, GISS-E2-R, MIROC-ESM, and MRI-CGCM3), this excessive ice cover reaches what is at present the Atlantic coast.

The LGM/PI annual mean precipitation anomalies vary significantly among models for this area (Figs. 3a and 3f). While some of the climate models show a precipitation increase by up to 50 % at 52° S when compared to the PI climate, other models suggest much drier conditions in the same area (up to -50 %). Regarding near-surface air temperatures, we observe a uniform range of LGM-PI anomalies, with most climate models suggesting averaged values within the range of -8 °C to -6 °C (Figs. 3b,f). In this region, CCSM4 and MRI-CGCM3 exhibit the coldest conditions relative to the PI, while displaying precipitation increases of up to 20 %. This combination of climate conditions leads to a strong ice sheet advance towards and beyond the eastern margins of the PATICE reconstruction. Ensemble members that reproduce a reasonable extension require LGM-PI temperature anomalies of around -6 °C, combined with a dry LGM/PI precipitation anomaly of about -20 % (Fig. 3f, see climate models AWI-ESM, MIROC-ES2L, MPI-ESM).

3.2 Low sensitivity of ice sheet extents to climate uncertainty in mid-Patagonia

Between 42° S and 52° S the model ensemble show a relatively low sensitivity to the climatic uncertainty provided by the PMIP models used in this study. Between 44° S and 52° S, a continuous ice sheet build-up is reached by most ensemble members, with an overall good match along both the eastern and western margins constrained by the PATICE data. Although temperature and precipitation anomalies at these latitudes show a large dispersion, ranging from -9 to -3 °C (LGM-PI) and from -30 to 25 % (LGM/PI), respectively (Fig. 3e), this does not lead to drastic changes in the resulting ice sheet extents. However, differences can be observed when comparing the modelled ice sheet thickness under different climate regimes. Under colder (LGM-PI) and wetter (LGM/PI) conditions, the modelled mean ice thickness of PIS increases. In the opposite case of warmer (LGM-PI) and drier (LGM/PI) conditions, the modelled mean thickness decreases.

This is in stark contrast with the relative performances of these models north of 44 °S, where climate conditions provided by COSMOS-ASO, IPSL-CM5A-LR and AWI-ESM-1-1-LR are only able to build fragmented ice structures (Figs. 2c,f,j), with the main body of the ice sheet not advancing further north of $\sim$ 44° S. The resulting ice sheet temperatures are linked to a temperature anomaly (LGM-PI) threshold equal or colder than -5 °C and a precipitation ratio (LGM/PI) of at least 1. These thresholds establish the minimum conditions needed to promote PIS advance north of 44º S (Figs. 3a,b,d,e).

3.3 Drivers of model failure in northern Patagonia

The PIS growth towards its northern confines is not uniformly captured by the ensemble. Most of the PMIP climate products tested here do not allow for an ice sheet expansion north of 42° S (Fig. 2), while the geologically constrained northern ice sheet margin is placed at 38° S. As stated earlier, positions of the former PIS margins derived using the INM-CM4-8 and MPI-ESM1-

https://doi.org/10.5194/cp-2023-47
Preprint. Discussion started: 16 June 2023


Climate of the Past Discussions

2-LR products are closer to those inferred from the PATICE data set. Although the forcing from AWI-ESM-1-1-LR enables an ice-covered area close to the reconstructed northern boundary (similar to the resulting ice extents from the MPI-ESM1-2-LR ensemble member), the ice cover produced by this simulation cannot qualify as an ice sheet north of 44° S, but rather as an isolated ice cap (Fig. 2j). Towards the northernmost part of the geologically constrained PIS extent (north of 40° S), none of the ensemble members is able to reproduce the reconstructed ice cover. However, a few ice bodies resembling ice caps are generated by the simulations driven by GISS–E2-R and MPI-ESM-P (Figs. 2e,h).

Between 40° S and 42° S, the INM-CM4-8 model showcases a pronounced reduction in precipitation rates during the LGM relative to the PI, reaching a -40 % drop at around 40° S, leading to significantly drier LGM conditions (Fig. 3a). This contrasts all other climate simulations (from both PMIP3 and PMIP4), in which LGM precipitation rates are either equal to or even larger than (up to 10 %) their corresponding PI values (Figs. 3a,d). Despite these significantly wetter conditions (25 to 50 % larger precipitation rates than in the INM-CM4-8 model), these ensemble members fail to initiate an ice sheet in this region. In the same range of latitudes, most PMIP3 and PMIP4 models show LGM-PI temperature anomalies ranging from -3 to -6 °C, while INM-CM4-8 infers a much larger temperature anomaly, reaching a value of -11 °C around 40° S. However, this anomaly suddenly decreases towards the northernmost margin of the PIS, preventing ice sheet growth there under precipitation-starved conditions (Figs. 3b,d). In this part of Patagonia, climate forcings from INM-CM4-8 and MPI-ESM1-2-LR thus stand out as the only PMIP model products providing atmospheric conditions that enable the growth of an ice sheet in agreement with the PATICE data set.

Our results highlight the critical role of regional air temperatures in the inception and expansion of the PIS over the northern sectors. On the one hand, drier but colder climate states are able to provide a set of conditions that promote ice sheet advance. On the other hand, wetter but warmer climates (i.e., mean annual anomaly of around -7 °C) tend to prevent ice accumulation despite relatively high rates of precipitation. These findings underline the importance of reduced modelled temperature biases as a prerequisite for robust model-based reconstructions of the Patagonian glacial history.

Our results suggest that in order to enable a PIS build-up north of 40º S that matches the PATICE reconstruction, mean annual temperature anomalies (LGM-PI) of at least -5 °C and precipitation ratios (LGM/PI) close or above to 1 are required. Although some of the climate models exhibit much wetter conditions during the LGM –with precipitation rates being up to 30 % higher than during the PI in this region (Fig. 3)–, they also produce smaller anomalies in temperatures (-2 °C to -4 °C, see Figs. 3a-c). Such climate conditions appear too warm to maintain a positive surface mass balance, thus prohibiting ice sheet inception or advance. In this context, the combination of near-surface air temperatures and precipitation rates from GISS-E2-R seems to define an absolute minimum threshold for the presence of an ice sheet in northern Patagonia.

4 Discussion

In this section, we first examine the correspondence between the PMIP paleoclimate model experiments and available constraints from empirical paleoglacial and paleoclimate evidence across Patagonia. In this context, we focus on quantifying whether model-based climate reconstructions are consistent with the reconstructed Patagonian ice sheet geometry over dif-

https://doi.org/10.5194/cp-2023-47
Preprint. Discussion started: 16 June 2023

Climate of the Past Discussions
Open Access
EGU

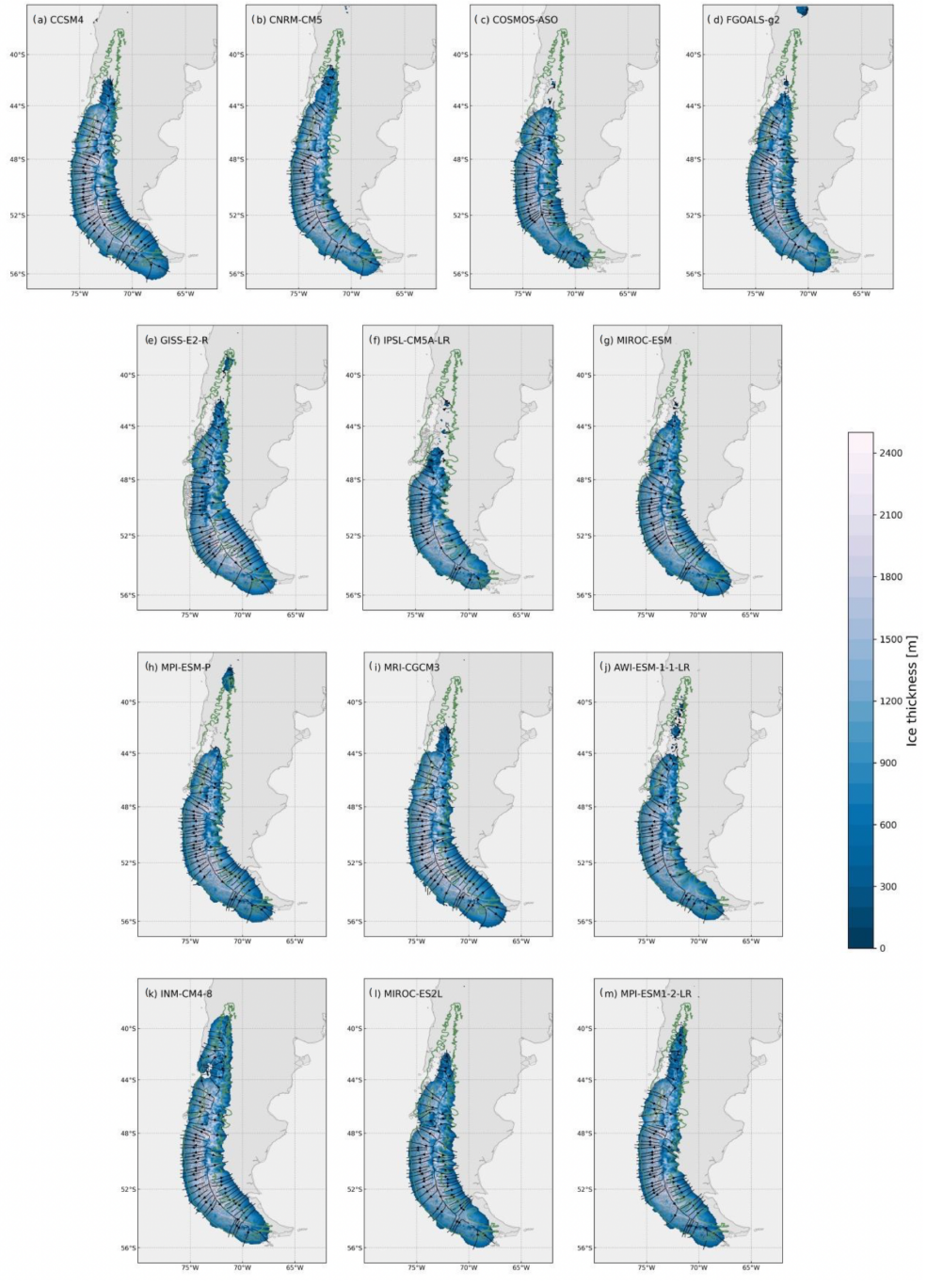

Figure 2. Modelled thickness of the PIS (m) and ice base velocity streamlines for the LGM. The green line shows the reconstructed glacier extent from the empirical evidence at 20 ka (Davies et al., 2020). The present-day coastline is shown for reference.

https://doi.org/10.5194/cp-2023-47
Preprint. Discussion started: 16 June 2023


Climate of the Past Discussions

ferent sectors of formerly glaciated Patagonia. Then, we identify potential impacts of the prescribed topographic forcing and horizontal climate model resolution on the modelled climate conditions. Finally, we discuss our findings in the context of asynchronous glaciation histories between the PIS and paleo ice sheets in the northern hemisphere, considering the limitations arising from the assumption of an ice sheet equilibrium with the climate of the Last Glacial Maximum (LGM).

4.1 Performance of PMIP models in Patagonia: Phase 3 versus Phase 4

Here, we take a closer look at the PMIP models and their regional behaviour across Patagonia, zooming in on the differences between the reconstructed monthly mean temperatures and precipitation rates. Some of the largest differences between model performance in the two phases of PMIP are related to the fact that PMIP3 anomalies show stronger cooling during the austral winter and weaker cooling during summer which tend to accentuate the amplitudes of the annual temperature cycle (Fig. 4). This is in contrast with the outputs of individual PMIP4 experiments, where MPI-ESM1-2-LR has similar characteristics to PMIP3 models, while MIROC-ES2L produces stronger negative temperature anomalies during the summer-early autumn period (January-April). In contrast, precipitation ratios show a high dispersion across seasons and models. In general, most models exhibit a general decrease in precipitation, particularly in the mean annual rates, even though some models infer an increase in winter precipitation. The exception is CNRM-CM5, which shows a general, albeit relatively small increase in both mean annual and winter precipitation rates.

When looking at the sub-regional (sector-scale) performance of PMIP climate, it becomes clear that most of them fail to reproduce the reconstructed extents of the northernmost sectors of the PIS during the LGM (38-42° S). To investigate the origin of this behaviour, we have calculated average temperature and precipitation anomalies within the former PIS outlines between 38° S and 42° S (Fig. 5). Large differences can be observed in the climate model reconstructions when looking at their particularities in this region. The models AWI-ESM-1-1-LR, INM-CM4-8 and MPI-ESM1-2-LR suggest larger negative temperature anomalies during the melting season. In particular, INM-CM4-8 stands out by producing very cold conditions during the LGM nearly throughout the entire year, with a higher amplitude during January and February (austral summer). Its drop in near-surface temperatures of around 12 °C during the melting season is an outlier, showing a difference of at least 4 °C relative to other PMIP4 models. Lower temperatures inferred from INM-CM4-8 act as a driving mechanism for the realistic ice sheet growth between 38-42° S. The temperature anomaly suggested by INM-CM4-8 is less intense during winter months, being closer to the range of inferred from the other models.

MIROC-ES2L produces the smallest LGM-PI temperature anomaly among all PMIP4 models, with an annual mean of around 4 °C. While MPI-ESM1-2-LR and AWI-ESM-1-1-LR reproduce relatively similar annual cycles, MPI-ESM1-2-LR provides 0.5 °C colder temperatures in the annual mean (Fig. 5. In contrast, PMIP3 models show two types of patterns - one similar to PMIP4 models and another with pronounced cooling. The first group of experiments (GISS-E2-R, IPSL-CM5A-LR, and MPI-ESM-P) results in smaller temperature anomalies between the LGM and PI summers, while other models show a greater cooling during the winter, with some having larger cooling amplitudes (e.g. CCSM4 and MRI-CGCM3).

Regarding the reconstructed precipitation rates, PMIP3 and PMIP4 exhibit significant differences. It is apparent that no common mean-annual precipitation patterns can be revealed (Fig. 3). Most models predict months with positive or negative anoma-

https://doi.org/10.5194/cp-2023-47
Preprint. Discussion started: 16 June 2023

Climate of the Past Discussions
Open Access
EGU

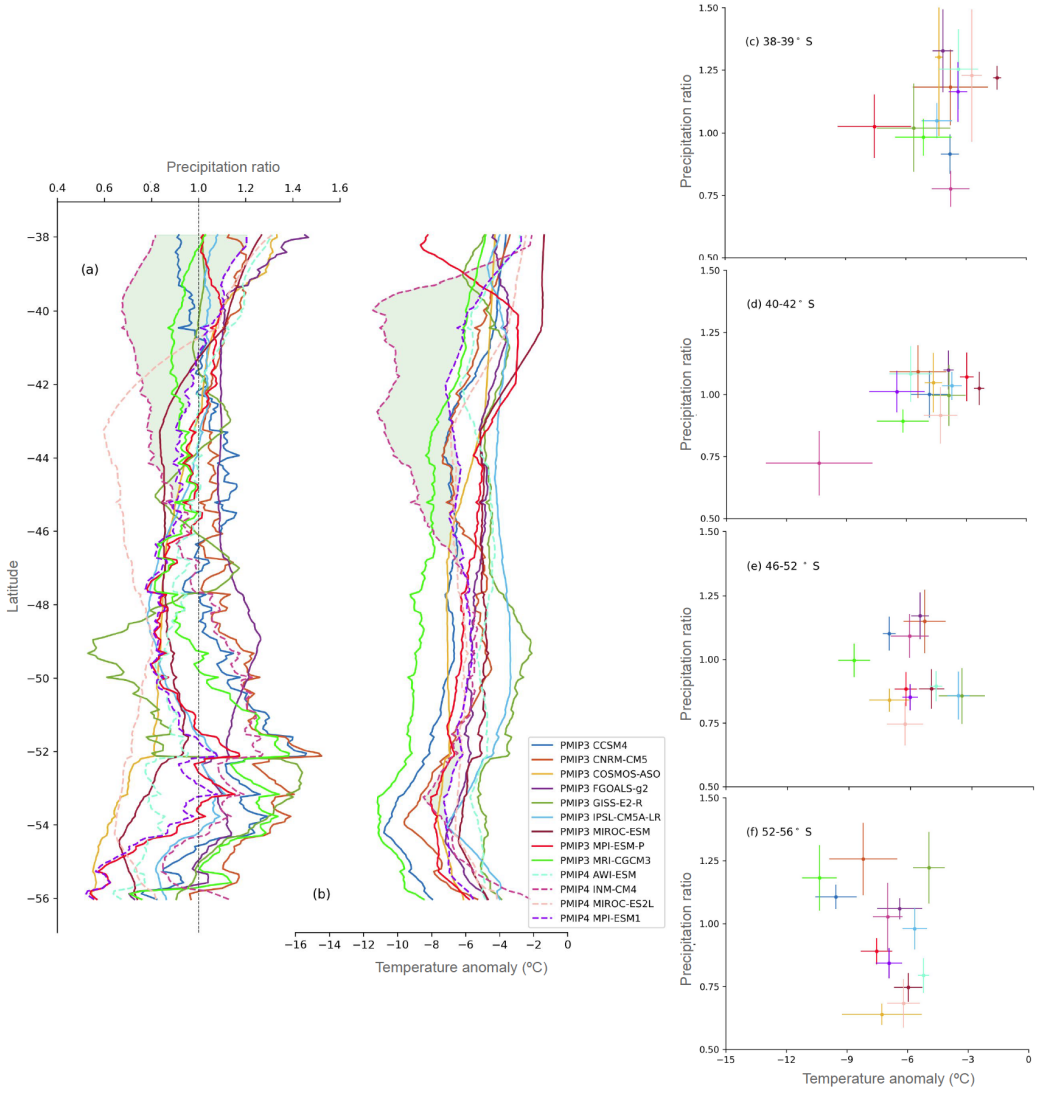

Figure 3. Latitudinal annual means of a) the LGM/PI precipitation ratio and b) temperature anomaly within the geologically reconstructed area of the former PIS (LGM-PI) (Davies et al., 2020). Shaded areas show the envelopes between the INM-CM4-8 and MPI-ESM1-2-LR. Annual mean precipitation ratio and temperature anomalies, including mean annual standard deviation through the year between c) 38° S and 39° S, d) 40° S and 42° S, e) 46° S and 52° S and f) 52° S and 56° S.

https://doi.org/10.5194/cp-2023-47
Preprint. Discussion started: 16 June 2023

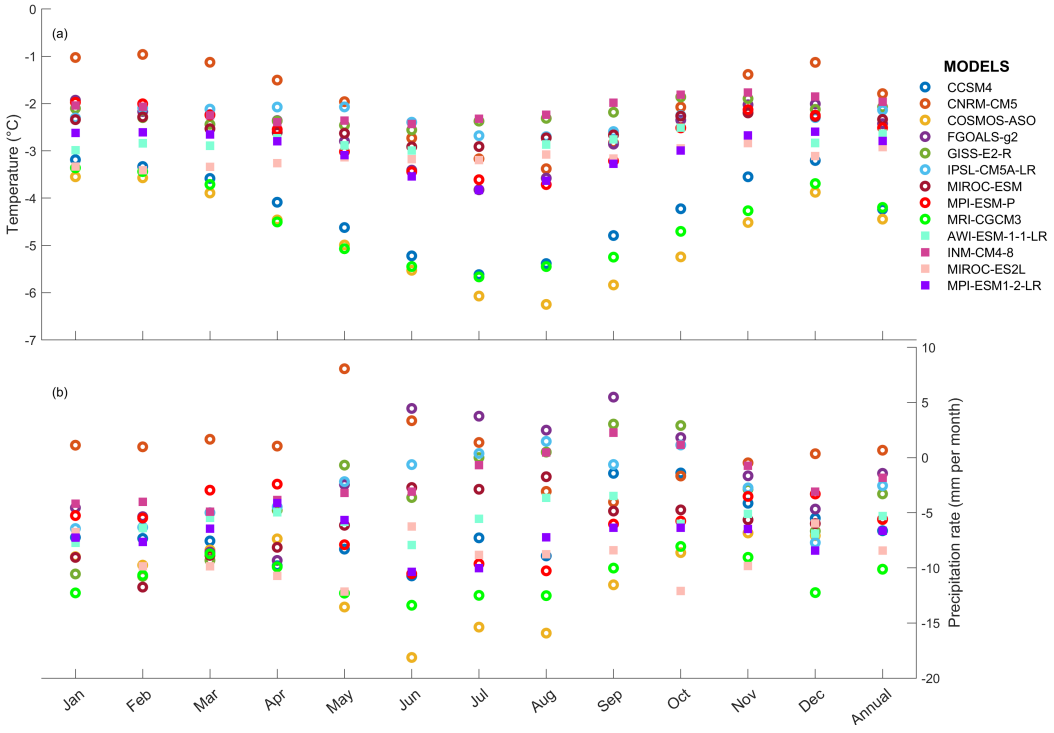

Figure 4. LGM-PI temperature anomalies (upper panel) and precipitation anomalies (bottom panel) for the monthly outputs of CMIP5-PMIP3 and CMIP6-PMIP4 averaged over the study zone.

lies throughout the year, except for INM-CM4-8, MIROC-ES2L, and MRI-CGCM3, which consistently generate lower-than-PI precipitation ratios for all months that are close to the lowest end of the total range. All other models tested here exhibit an overall increase in the annual mean precipitation rates in this region, with CNRM-CM5 and FGOALS-g2 generating the wettest conditions among all models.

As we show in Sect. 3, the models that produce the most realistic modelled extents of the PIS between 38-42° S are those that exhibit the strongest negative LGM-PI temperature anomalies (-8 to -12 °C) during the melting season. These models are INM-CM4-8 and MPI-ESM1-2-LR, although the northward ice sheet advance resulting from the latter only reaches 40° S (Figs. 2k,l), leaving the formerly PIS-covered territories between 38° S and 40° S ice-free. This is because the (LGM-PI) temperature anomaly derived from MPI-ESM1-2-LR is at least 4 °C lower than in INM-CM4-8, which displays a drastic drop in the temperature anomaly (between -12 °C and -10 °C) towards the north of Patagonia (Fig. 3b).

Paleo-vegetation records at 41° S infer 6 to 7 °C colder mean annual temperatures during the LGM than at present (Moreno et al., 1999). When these reconstructions are combined with the glacial geology and palynology data collected within 40-42° S, we arrive at a range of 6 to 8 °C colder mean summer temperatures and 6 to 7 °C colder mean annual temperatures at LGM (Denton et al., 1999). On the one hand, these data suggest that the cooling of $\sim$ 12 °C observed in INM-CM4-8 during summer months is relatively extreme compared to the range observed in existing proxy records. On the other hand, the AWI-ESM-1-1-

https://doi.org/10.5194/cp-2023-47
Preprint. Discussion started: 16 June 2023

Figure 5. LGM-PI temperature anomalies (upper panel) and precipitation anomalies (bottom panel) for the monthly output of CMIP5-PMIP3 and CMIP6-PMIP4 calculated of the northernmost sector of the former PIS. Calculations are made over the grid points that match the reconstructed PIS extents by Davies et al. (2020) within the 38-42° S study zone.

LR and MPI-ESM1-2-LR models arrive at summer anomalies that are consistent with the constrained range. However, annual mean temperature anomalies in these two models are close to -5 °C, which is 1 °C below the lower limit of the suggested range (Fig. 3d). By comparison, INM-CM4-8 infers a value of around -8 °C, which overestimates the reconstructed cooling by 1 °C. Nevertheless, among all models tested in this study, AWI-ESM-1-1-LR, INM-CM4-8 and MPI-ESM1-2-LR produce temperature anomalies that are closest to the available paleoclimatic records in northern Patagonia.

It is difficult to infer what factors are responsible for this regional scattering between different phases of PMIP, mainly due to the number of changes between model versions, e.g., the treatment of vegetation, atmospheric dust loading, and prescribed ice thickness and topography (Kageyama et al., 2017). The latter, in particular, raises questions about the importance of the PIS for shaping regional climate regimes during the LGM and its impact on modelled atmospheric states. This highlights a need for studies providing a benchmark for the effects of topographic and albedo feedbacks (among others) between the PIS and the regional climate dynamics.

Previously, Yan et al. (2022) modelled the PIS during the LGM using climate forcing products from phases 2, 3 and 4 of the PMIP project. To achieve a good fit with geological evidence, the PDD factors in the surface mass balance (SMB) model were reduced to promote ice sheet growth. However, the applied PDD factors in this earlier study are not supported by existing

https://doi.org/10.5194/cp-2023-47
Preprint. Discussion started: 16 June 2023


Climate of the Past Discussions

studies of present-day ice sheets (Peano et al., 2017; Seroussi et al., 2020) or ice fields in Patagonia (Möller and Schneider, 2008; Bown et al., 2019), indicating that this evaluation may be biased due to the choice of model parameters. The best fit with the reconstructed ice sheet configuration in Yan et al. (2022) was achieved using MPI-ESM1-2-LR output, while the forcing using INM-CM4-8 resulted in a much larger PIS. Our findings indicate that using a set of model parameters that is consistent with the current knowledge leads to an underestimation of ice sheet extent in the north of Patagonia, as observed in the experiment driven by MPI-ESM1-2-LR, while the climate conditions from INM-CM4-8 still allow for a more extensive ice coverage, albeit with a less over-expansion.

4.2 Impacts of topography and resolution

In Sect. 3 we show that, under the chosen parameters (Table 1), none of the experiments carried out in this study were able to build an ice sheet in agreement with the reconstructed PIS geometry (Fig. 2). It has become clear that all PMIP models struggle to reproduce air temperatures that are consistent with both local proxy records and geological reconstructions of the former ice sheet extents in northern Patagonia (Figs. 3b,c,d). Due to the fact that the northern sector of the PIS is a relatively narrow ice mass that resided in an area of exceptionally steep topography (Fig. 6), here we analyse to which extent this important factor for the ice sheet growth is reproduced by the PMIP climate models, and whether the typical lack of resolution in global models may be a possible origin of such a struggle. Furthermore, the ice sheet forcing itself is an important component of paleo experiments, introducing regional-scale climate feedback through additional topographic barriers and the albedo effect (Löfverström et al., 2014; Beghin et al., 2015; Liakka et al., 2016). In this context, it is important to note that participants of PMIP used different ice sheet forcings in different project phases: the PMIP3 ice sheet reconstruction (Abe-Ouchi et al., 2015), the ICE-6G_C (Peltier et al., 2015) and GLAC-1D (Tarasov et al., 2012). All these reconstructions are sufficiently different from each other, leading to deviations in climate model results (Abe-Ouchi et al., 2015). In addition, dissimilar horizontal resolutions within climate models may induce further differences in modelled climate regimes on a regional scale (Table 2). Here we focus on the analysis of PMIP4 topographic forcings and the differences between them. We expect that our observations and conclusions based on the analysis of PMIP4 models will be broadly applicable to other phases of PMIP, except that most of the earlier PMIP phases did not include an ice sheet forcing in Patagonia (Kageyama et al., 2017).

PMIP4 models used in this study apply dissimilar topographic forcings, mainly due to modifications to meet the spatial resolution imposed in each of them. In Patagonia, all models include simplified topographic features that do not exceed 1500 m in altitude (Fig. 6). Furthermore, these simplifications shift the position of the Andes and flatten the observed topography, which exceed 3000 m above sea level in the north (Fig. 1). Regardless of its good ice-covered area agreement against PATICE, the topographic forcing of INM-CM4-8 (which has the finest latitudinal resolution among PMIP4 climate models) has undergone visible substantial modifications (Fig. 6). INM-CM4-8 does feature a higher topography in the northern part of the model domain, where it might accentuate colder and drier LGM climate conditions. This suggests that a much higher spatial resolution is needed to capture the atmospheric dynamics and climate gradients over the complex terrain and extreme environment of the Andes when using general circulation models (Bozkurt et al., 2019).

To compare the ice sheet thickness and ice-covered area of each PMIP4 ensemble member, we compute the difference between

https://doi.org/10.5194/cp-2023-47
Preprint. Discussion started: 16 June 2023

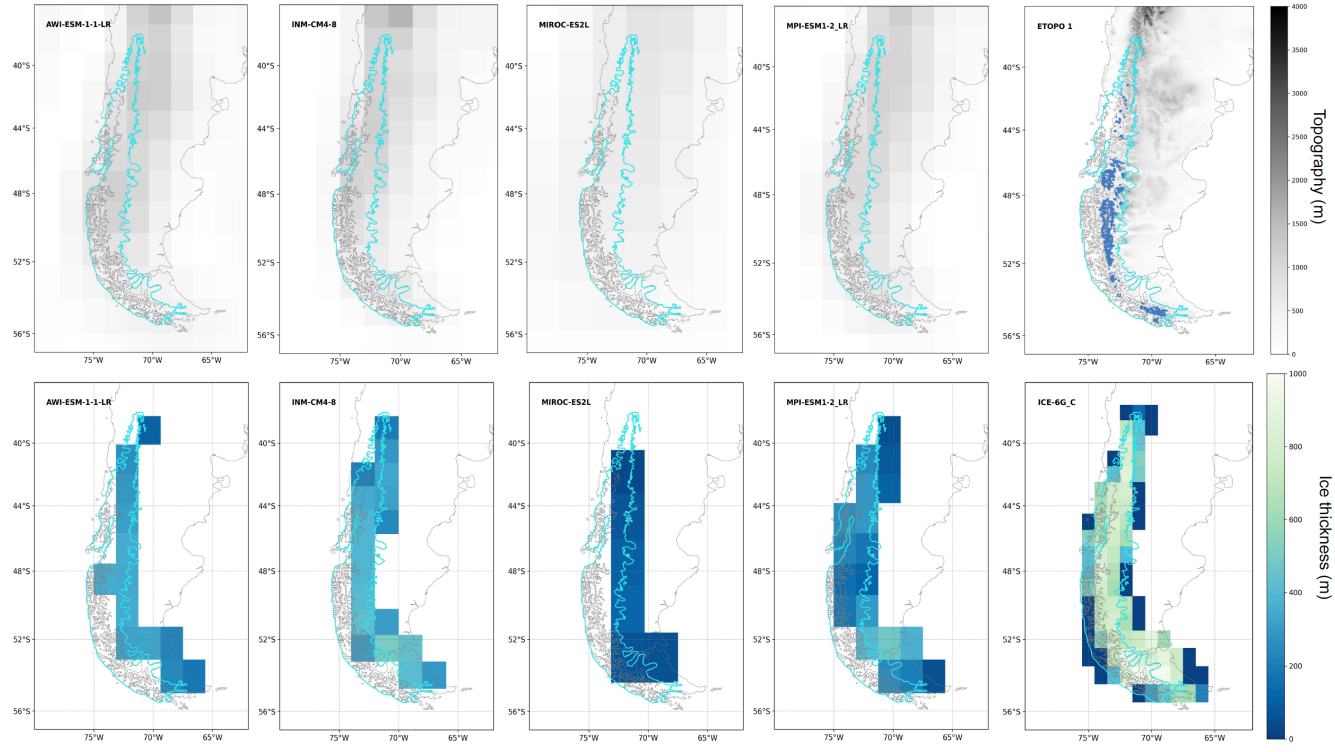

Figure 6. Prescribed topography (upper panel) and ice thickness (bottom panel) by the PMIP4 models considered in this study. Etopo-1 (Amante and Eakins, 2009) and the ICE-6G_C reconstruction (Peltier et al., 2015) included as of the ice sheet forcings in PMIP4. The Cyan line shows the PIS extension for the 20 ka (Davies et al., 2020). Present-day ocean-continent limits are shown for interpretation.

the LGM and the PI topographies assuming that the sea level during LGM was 120 m lower than present. The ice mask provided by each ensemble member is then used to delimit the ice sheet geometry. If we focus on the PMIP 4 models alone, we can observe that ice sheet geometries prescribed in the AWI-ESM-1-1-LR, INM-CM4-8 and MPI-ESM1-2_LR climate experiments are broadly consistent with the north-to-south extents of the former PIS derived from the geological evidence (Davies et al., 2020). This does not imply, however, that the prescribed PIS in any of these climate models is necessarily accurate (Fig. 6). This is particularly evident in the prescribed ice sheet within MIROC-ES2L, which is the coarsest climate model among the four PMIP4 models analysed that fails to reproduce LGM climate conditions that enable our ice sheet model to build an ice sheet extension consistent with PIS north of 44° S (Fig. 6).

Within the geologically constrained ice-covered area, our comparison of monthly anomalies in near-surface mean air temperatures reveals large discrepancies between the four PMIP4 models north of 46° S (Fig. 3b,c,d). INM-CM4-8 infers a more negative anomaly compared to the three other models, peaking at a mean annual value of nearly -12 °C at around 40° S. At this latitude INM-CM4-8 prescribes an ice thickness of around 300 m (Figs. 5 and 6), whereas MIROC-ES2L does not include any ice sheet forcing in this area. As a consequence, the latter generates much higher mean annual temperatures, with an LGM-PI

https://doi.org/10.5194/cp-2023-47
Preprint. Discussion started: 16 June 2023

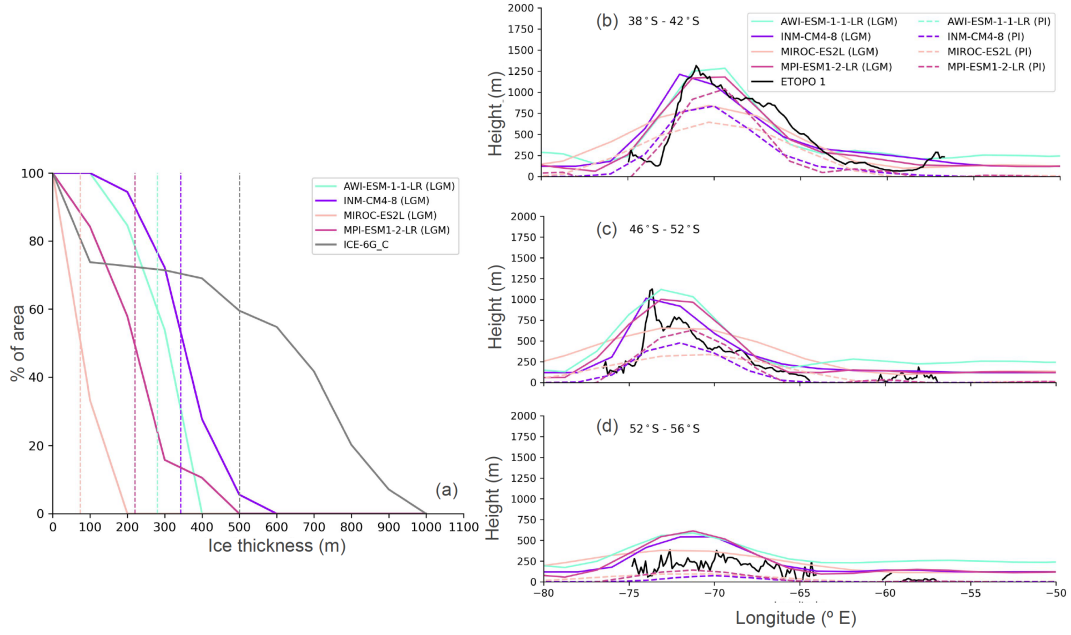

Figure 7. (a) Hypsometric curves of prescribed ice forcings in the PMIP4 models against the reference ICE-6G_C geometry. Mean ice thickness for each model is shown in vertical lines. Mean topography between (b) 38º S to 42º S, (c) 42º S to 52º S and (d) 52º S to 56º S. The PMIP4 topography of each member is shown in dashed and continuous lines for its PI and LGM time periods, respectively.

anomaly amounting to only -3 °C. This implies that in this geographical sector, the two models placed at the extreme ends of the spectrum of possible regional thermal climate regimes are separated by 9 °C. Although AWI-ESM-1-1-LR and MPI-ESM1-2-LR have relatively similar ice sheet boundary conditions at these latitudes when compared to INM-CM4-8, they both arrive at smaller temperature anomalies north of 42° S, leading to a limited expansion of the PIS and ice sheet fragmentation (Fig. 2).

Our simulations suggest that most PIS sectors had an ice thickness between 1000 and 1500 m, with a maximum close to 2000 m. Such thick ice cover should have greatly impacted regional climate conditions during the LGM. In one of the most problematic regions, located between 38° S to 42° S, PMIP experiments prescribe an ice sheet that peaks at a thickness of around 300 m, while our experiments suggest a likely range of thickness values between 200 and 700 m over this area. However, it appears difficult to constrain the regional ice sheet thickness and extent using geological reconstructions that are very fragmented and lack direct constraints on the former ice surface elevations (Boex et al., 2013; Troch et al., 2022).

Towards the south-eastern sectors of the PIS, our results showcase a consistent overestimation of modelled ice sheet extents relative to the geological evidence. We partially attribute this excessive ice sheet growth to the mismatch between the reconstructed PIS coverage and the prescribed topography in the climate models: ice sheets invade formerly ice-free territories, potentially promoting extra cooling and leading to reduced ablation. The rather poor performance of climate models along leeward slopes of the Andes can be therefore partly attributed to unrealistic ice sheet forcings that lost their outlines and spatial

https://doi.org/10.5194/cp-2023-47
Preprint. Discussion started: 16 June 2023


Climate of the Past Discussions

details during spatial upscaling. Other potential contributing factors to this unrealistic ice sheet growth in the south-east include erroneous albedo forcings and a lack of orographic effects due to unresolved precipitation barriers (Fig. 7b,c,d). Erroneous representation of the orographic effect on precipitation is very likely a contributor to the mismatches between the modelled and reconstructed ice sheets in this area due to very strong flattening of the topographic forcing (including mountain ranges and prescribed ice sheets), and thus its inability to impose the rain-shadow effect under these horizontal resolutions (Lofverstrom and Liakka, 2018; Bozkurt et al., 2019; Almazroui et al., 2021). The lack of this effect leads to reduced precipitation on the windward side but much higher precipitation on the leeward side of the Andes, promoting the growth and eventually overflow of the PIS beyond its geologically constrained eastern margin.

Studies of former ice masses in the Northern Hemisphere have been used to demonstrate that under the same orbital and greenhouse forcings, discrepancies between ice sheet boundary conditions in otherwise identical experiments lead to robust, large-scale impacts on the atmospheric circulation and temperature (Ullman et al., 2014; Löfverström et al., 2014; Bakker et al., 2020; Izumi et al., 2023). The PMIP models are able to reproduce the general temperature and precipitation conditions over South America during the LGM (Berman et al., 2016). However, due to their resolution they are unable to reproduce regional climate responses with a necessary detail (Bozkurt et al., 2019). As we have shown, their resolution is generally too coarse to drive modelling studies of the narrow ice sheet in Patagonia since. We strongly suggest that a significantly higher climate model resolution is needed to study the influence of the Andean topography features on the past regional climate dynamics and capture the longitudinal gradient between the colder and wetter windward side of the Andean mountain range and the less cold and drier leeward side. Based on this analysis, we suggest that all PMIP models currently oversimplify the terrain in our target area, distorting the land topography through smoothing, flattening and by prescribing too thin and incorrectly distributed ice cover, with a maximum ice sheet thickness reaching between 700 and 800 (Fig. 7a) m as opposed to the expected thickness of up to 2000 m (Fig. 2).

To summarize, climate models show poor performance both in the south-eastern sector of the former PIS and at its northern tip. On the one hand, the south-eastern sector reveals an excessive ice sheet growth amounting to up to 400 m thick undocumented ice masses in formerly ice-free regions. On the other hand, the northern sector of the PIS is lacking ice, partly due to thinner or non-existent ice sheet boundary conditions in PMIP4 climate experiments and too warm climate regimes inferred from most PMIP experiments.

4.3 Potential implications of dissimilar LGM timings in the Southern and Northern Hemispheres

Here we discuss the limitations of our study design and propose possible ways of overcoming these in future work. The first challenge in this study is related to the assumption of climate and ice sheet equilibrium states during the global LGM. It is however an open question whether it is fair to generate PIS model reconstructions assuming that the ice sheet was in a steady-state under global LGM climate conditions, and if not, how to treat the lack of reliable climate forcing for the earlier periods of the last glacial cycle. The second challenge is related to the interpretation of major planetary drivers that enabled an asynchronous glacial response of the two hemispheres to changes in the orbital and greenhouse gas forcings (Doughty et al., 2015).

The geologically-constrained gap between local LGM timings in Patagonia and different parts of the Northern Hemisphere

https://doi.org/10.5194/cp-2023-47
Preprint. Discussion started: 16 June 2023


Climate of the Past Discussions

raises an important question about the drivers of these differences in timing. These drivers potentially involve climatic feedback mechanisms, hemispheric climate sensitivities to orbital and greenhouse gas forcings and interactions between the two hemispheres (Darvill et al., 2016). The current evidence suggests that the local glacial peak in the southern Andes and Patagonia happened at about 35 ka (Zech et al., 2011; Davies et al., 2020), which is much earlier than local LGM inferred for most of the paleo ice sheets in the Northern Hemisphere. Aside from the Barents-Kara Sea Ice Sheet and smaller glaciations in Asia, ice masses of the last glacial cycle attained their maximum extents and were driven towards maximum ice volumes during the Marine Isotope Stage 2, at about 24-18 ka, (Hughes et al., 2016; Patton et al., 2016; Gowan et al., 2021) by a strong cooling between 30 and 20 ka. According to the current state of knowledge, these massive ice sheets only began disintegrating at around 18 ka (Patton et al., 2017; Stokes, 2017; Gowan et al., 2021). The situation is however different for the Southern Hemisphere. Due to a lack of large-scale paleo ice sheets and scarce information about past fluctuations of the Antarctic Ice Sheet, it is necessary to look at the existing evidence for the advance and retreat history of smaller ice bodies in order to contextualise the situation in the Southern Hemisphere during the last glacial cycle. For example, records coming from an icefield located in the Southern Alps in New Zealand indicate that this ice mass reached its maximum extent at around 28 ka (Rother et al., 2014). According to recent studies, its growth towards 28 ka was influenced by a slight decrease in temperatures in the preceding two millennia (Darvill et al., 2016). The reconstructed air temperature cooling at this location is estimated as 6 to 6.5 °C below present, accompanied by a precipitation reduction of up to -25 % (Golledge et al., 2012b). During the period between 26 to 20 ka, this icefield is thought to have undergone a slow and continuous retreat, followed by a standstill at around 19 ka. This coincides with the time when most of the Northern Hemisphere ice sheets began retreating from their maximum positions due to slowly increasing solar radiation and activation of positive climate feedback mechanisms. Arguably, the Antarctic Ice Sheet seems to have been stable until about 18 ka, after which it experienced an increase in air temperatures synchronised with the increase in CO_2 concentrations (Parrenin et al., 2013; Brook and Buizert, 2018). This triggered the retreat of ice margins in Antarctica, New Zealand, and South America, where the PIS experienced an accelerated retreat starting from 18 ka (Davies et al., 2020). The current evidence of an early local LGM in Antarctica is inconclusive, partly due to an extreme sensitivity of the Antarctic Ice Sheet to the ocean forcing as opposed to the thermal atmospheric forcing playing the largest role in the deglaciation of formerly ice sheet-covered areas (Golledge et al., 2012a). However, pieces of evidence from Patagonia and New Zealand suggest that the Southern Hemisphere might have responded very differently to the global cooling of the last glacial period compared to the Northern Hemisphere (Darvill et al., 2016; Shulmeister et al., 2019).

5 Conclusions

We have performed a regional assessment of the PMIP paleoclimate model products (phases 3 and 4) across Patagonia using a combination of ice sheet modelling, paleoglacial reconstructions, and paleoclimate proxy data as a metric for climate model performance. As part of this assessment, we have narrowed down the range of atmospheric conditions needed during the LGM to promote an inception and advance of the PIS in its different sectors, so that they are in agreement with the ice sheet-wide empirical reconstruction PATICE. For this purpose, we have designed an ensemble of large-scale ice sheet model simulations

https://doi.org/10.5194/cp-2023-47
Preprint. Discussion started: 16 June 2023

driven by downscaled PMIP climate products to obtain PIS configurations that are in equilibrium with each model-based climate regime. This set of ice sheet model simulations has been used to analyse and interpret the characteristics of contrasting regional climate regimes from ensemble members across different latitudinal sectors of Patagonia.

We have observed that most paleoclimate models provide much warmer atmospheric conditions along the northern segment of the former PIS than those required to initiate the growth of an ice sheet and support its advance towards the geologically reconstructed boundaries. Our analysis indicates that a sector-averaged mean temperature anomaly of at least 5 °C below the present-day conditions is needed to generate an ice cover that matches the geological evidence.

At the northernmost tip of the PIS, we find a relatively narrow envelope of PMIP-derived temperature and precipitation anomalies that accommodates a reasonable agreement between the modelled and reconstructed PIS extents. The warmest climate regimes within this envelope correspond to a minimum cooling of approximately -7 °C accompanied by wetter-than-present conditions with a precipitation increase of around 15 %. The coldest and driest end of the plausible range is associated with a more significant cooling of -11 °C and a reduction in precipitation rates of around 20% to keep the ice sheet from excessive expansion.

Between 44° S and 52° S, most ensemble members show a continuous build-up of the PIS, which is in general agreement with the reconstructed eastern and western ice sheet margins at the LGM. We have constrained an envelope of the LGM-PI temperature anomalies within this region to a range of -5 to -8 °C that is accompanied by the range of precipitation rates anomalies between -20 % and 20 % relative to their PI counterparts. In sharp contrast to the results for the northern and southern boundaries, climate models exhibit an overall high degree of agreement within this broad PIS sector.

Finally, in the southernmost sector of the former PIS (between 52° S and 56° S), our results showcase a consistent overestimation of the ice sheet extents relative to the geological reconstruction. Our analysis indicates that most of the PMIP models simulate climate conditions that are too cold to produce significant surface ablation. In the absence of any other factors that can limit the ice sheet advance (other than processes such as calving at the coast), this excessive accumulation promotes a slow but steady ice sheet growth, eventually causing the modelled ice sheet to overflow its reconstructed geographical limits. We hypothesise that a higher climate model resolution and significantly better resolved topographic boundary conditions are needed to capture the longitudinal gradients across the Andes.

Code and data availability. SICOPOLIS is a free and open-source software. Details of its implementation can be found at http://sicopolis.net (last access 8th of June, 2023). The PMIP output used in this study can be found on the Earth System Grid Federation website, in particular, CMIP5-PMIP3 (https://esgf-node.ipsl.upmc.fr/search/cmip5-ipsl) and CMIP6-PMIP4 (https://esgf-node.ipsl.upmc.fr/search/cmip6-ipsl). Data will be available once the manuscript has been accepted for publication through zenodo repository

https://doi.org/10.5194/cp-2023-47
Preprint. Discussion started: 16 June 2023

Author contributions. ACL and FRR have contributed equally to this work. The original concept has been conceived by FRR under the supervision of IR and has been further developed by ACL, again under the supervision of IR, with inputs from all authors. All authors contributed to the writing process.

Competing interests. At least one of the (co-)authors is a member of the editorial board of Climate of the Past.

Acknowledgements. ACL acknowledges support from the Agencia Nacional de Investigacion y Desarrollo (ANID) Programa Becas de Doctorado en el Extranjero, Becas Chile for the doctoral scholarship. FRR acknowledges support from the "FONDAP 15110009" Centro de Ciencia del Clima y la Resiliencia (CR)2 (DGF-UChile) and the Ministerio de Educación, Fortalecimiento de la Investigación en Cambio Climático y Conservación Antártica y Subantártica (IES20992). This article is partially based on FRR's undergraduate thesis at the University of Concepcion under IR's and MJC's supervision.

https://doi.org/10.5194/cp-2023-47
Preprint. Discussion started: 16 June 2023

References

Abe-Ouchi, A., Saito, F., Kageyama, M., Braconnot, P., Harrison, S. P., Lambeck, K., Otto-Bliesner, B. L., Peltier, W., Tarasov, L., Peterschmitt, J.-Y., et al.: Ice-sheet configuration in the CMIP5/PMIP3 Last Glacial Maximum experiments, Geoscientific Model Development, 8, 3621–3637, https://doi.org/10.5194/gmd-8-3621-2015, 2015.

Almazroui, M., Ashfaq, M., Islam, M. N., Rashid, I. U., Kamil, S., Abid, M. A., O'Brien, E., Ismail, M., Reboita, M. S., Sörensson, A. A., et al.: Assessment of CMIP6 performance and projected temperature and precipitation changes over South America, Earth Systems and Environment, 5, 155–183, https://doi.org/10.1007/s41748-021-00233-6, 2021.

Amante, C. and Eakins, B. W.: ETOPO1 arc-minute global relief model: procedures, data sources and analysis, NOAA Technical Memorandum NESDIS NGDC-24, https://doi.org/10.7289/V5C8276M, 2009.

Annan, J. and Hargreaves, J. C.: A new global reconstruction of temperature changes at the Last Glacial Maximum, Climate of the Past, 9, 367–376, https://doi.org/10.5194/cp-9-367-2013, 2013.

Bakker, P., Rogozhina, I., Merkel, U., and Prange, M.: Hypersensitivity of glacial summer temperatures in Siberia, Climate of the Past, 16, 371–386, https://doi.org/10.5194/cp-16-371-2020, 2020.

Bartlein, P. J., Harrison, S., Brewer, S., Connor, S., Davis, B., Gajewski, K., Guiot, J., Harrison-Prentice, T., Henderson, A., Peyron, O., et al.: Pollen-based continental climate reconstructions at 6 and 21 ka: a global synthesis, Climate Dynamics, 37, 775–802, https://doi.org/10.1007/s00382-010-0904-1, 2011.

Beghin, P., Charbit, S., Dumas, C., Kageyama, M., and Ritz, C.: How might the North American ice sheet influence the northwestern Eurasian climate?, Climate of the Past, 11, 1467–1490, https://doi.org/10.5194/cp-11-1467-2015, 2015.

Berman, A. L., Silvestri, G. E., and Tonello, M. S.: Differences between Last Glacial Maximum and present-day temperature and precipitation in southern South America, Quaternary Science Reviews, 150, 221–233, https://doi.org/10.1016/j.quascirev.2016.08.025, 2016.

Bernales, J., Rogozhina, I., Greve, R., and Thomas, M.: Comparison of hybrid schemes for the combination of shallow approximations in numerical simulations of the Antarctic Ice Sheet, The Cryosphere, 11, 247–265, https://doi.org/10.5194/tc-11-247-2017, 2017.

Boex, J., Fogwill, C., Harrison, S., Glasser, N., Hein, A., Schnabel, C., and Xu, S.: Rapid thinning of the late Pleistocene Patagonian Ice Sheet followed migration of the Southern Westerlies, Scientific Reports, 3, 1–6, https://doi.org/10.1038/srep02118, 2013.

Bown, F., Rivera, A., Pętlicki, M., Bravo, C., Oberreuter, J., and Moffat, C.: Recent ice dynamics and mass balance of Jorge Montt Glacier, Southern Patagonia Icefield, Journal of Glaciology, 65, 732–744, https://doi.org/10.1017/jog.2019.47, 2019.

Bozkurt, D., Rojas, M., Boisier, J. P., Rondanelli, R., Garreaud, R., and Gallardo, L.: Dynamical downscaling over the complex terrain of southwest South America: present climate conditions and added value analysis, Climate Dynamics, 53, 6745–6767, https://doi.org/10.1007/s00382-019-04959-y, 2019.

Braconnot, P., Otto-Bliesner, B., Harrison, S., Joussaume, S., Peterchmitt, J.-Y., Abe-Ouchi, A., Crucifix, M., Driesschaert, E., Fichefet, T., Hewitt, C., et al.: Results of PMIP2 coupled simulations of the Mid-Holocene and Last Glacial Maximum–Part 1: experiments and large-scale features, Climate of the Past, 3, 261–277, https://doi.org/10.5194/cp-3-261-2007, 2007.

Braconnot, P., Harrison, S. P., Kageyama, M., Bartlein, P. J., Masson-Delmotte, V., Abe-Ouchi, A., Otto-Bliesner, B., and Zhao, Y.: Evaluation of climate models using palaeoclimatic data, Nature Climate Change, 2, 417–424, https://doi.org/10.1038/nclimate1456, 2012.

Brook, E. J. and Buizert, C.: Antarctic and global climate history viewed from ice cores, Nature, 558, 200–208, https://doi.org/10.1038/s41586-018-0172-5, 2018.

https://doi.org/10.5194/cp-2023-47
Preprint. Discussion started: 16 June 2023

Calov, R. and Greve, R.: A semi-analytical solution for the positive degree-day model with stochastic temperature variations, Journal of Glaciology, 51, 173–175, https://doi.org/10.3189/172756505781829601, 2005.

Darvill, C. M., Bentley, M. J., Stokes, C. R., and Shulmeister, J.: The timing and cause of glacial advances in the southern mid-latitudes during the last glacial cycle based on a synthesis of exposure ages from Patagonia and New Zealand, Quaternary Science Reviews, 149, 200–214, https://doi.org/10.1016/j.quascirev.2016.07.024, 2016.

Davies, B. J., Darvill, C. M., Lovell, H., Bendle, J. M., Dowdeswell, J. A., Fabel, D., García, J.-L., Geiger, A., Glasser, N. F., Gheorghiu, D. M., et al.: The evolution of the Patagonian Ice Sheet from 35 ka to the present day (PATICE), Earth-Science Reviews, 204, 103 152, https://doi.org/10.1016/j.earscirev.2020.103152, 2020.

Denton, G. H., Heusser, C., Lowel, T., Moreno, P. I., Andersen, B. G., Heusser, L. E., Schlühter, C., and Marchant, D. R.: Interhemispheric linkage of paleoclimate during the last glaciation, Geografiska Annaler: Series A, Physical Geography, 81, 107–153, https://doi.org/10.1111/1468-0459.00055, 1999.

Doughty, A. M., Schaefer, J. M., Putnam, A. E., Denton, G. H., Kaplan, M. R., Barrell, D. J., Andersen, B. G., Kelley, S. E., Finkel, R. C., and Schwartz, R.: Mismatch of glacier extent and summer insolation in Southern Hemisphere mid-latitudes, Geology, 43, 407–410, https://doi.org/10.1130/G36477.1, 2015.

Evans, M. N., Tolwinski-Ward, S. E., Thompson, D. M., and Anchukaitis, K. J.: Applications of proxy system modeling in high resolution paleoclimatology, Quaternary science reviews, 76, 16–28, https://doi.org/10.1016/j.quascirev.2013.05.024, 2013.

Golledge, N. R., Fogwill, C. J., Mackintosh, A. N., and Buckley, K. M.: Dynamics of the last glacial maximum Antarctic ice-sheet and its response to ocean forcing, Proceedings of the National Academy of Sciences, 109, 16 052–16 056, https://doi.org/10.1073/pnas.1205385109, 2012a.

Golledge, N. R., Mackintosh, A. N., Anderson, B. M., Buckley, K. M., Doughty, A. M., Barrell, D. J., Denton, G. H., Vandergoes, M. J., Andersen, B. G., and Schaefer, J. M.: Last Glacial Maximum climate in New Zealand inferred from a modelled Southern Alps icefield, Quaternary Science Reviews, 46, 30–45, https://doi.org/10.1016/j.quascirev.2012.05.004, 2012b.

Gowan, E. J., Zhang, X., Khosravi, S., Rovere, A., Stocchi, P., Hughes, A. L., Gyllencreutz, R., Mangerud, J., Svendsen, J.-I., and Lohmann, G.: A new global ice sheet reconstruction for the past 80 000 years, Nature communications, 12, 1199, https://doi.org/10.1038/s41467-021-21469-w, 2021.

Greve, R.: Application of a polythermal three-dimensional ice sheet model to the Greenland ice sheet: response to steady-state and transient climate scenarios, Journal of Climate, 10, 901–918, https://doi.org/10.1175/1520-0442(1997)010<0901:AOAPTD>2.0.CO;2, 1997.

Greve, R. and Blatter, H.: Dynamics of ice sheets and glaciers, Springer Science & Business Media, https://doi.org/10.1007/978-3-642-03415-2, 2009.

Hamza, V. M. and Vieira, F.: Global heat flow: new estimates using digital maps and GIS techniques, International Journal of Terrestrial Heat Flow and Applied Geothermics, 1, 6–13, https://doi.org/10.31214/ijthfa.v1i1.6, 2018.

Harrison, S. P., Bartlein, P., Izumi, K., Li, G., Annan, J., Hargreaves, J., Braconnot, P., and Kageyama, M.: Evaluation of CMIP5 palaeosimulations to improve climate projections, Nature Climate Change, 5, 735–743, https://doi.org/10.1038/nclimate2649, 2015.

Holden, P. B., Edwards, N., Oliver, K., Lenton, T., and Wilkinson, R.: A probabilistic calibration of climate sensitivity and terrestrial carbon change in GENIE-1, Climate Dynamics, 35, 785–806, https://doi.org/10.1007/s00382-009-0630-8, 2010.

Hughes, A. L., Gyllencreutz, R., Lohne, Ø. S., Mangerud, J., and Svendsen, J. I.: The last Eurasian ice sheets–a chronological database and time-slice reconstruction, DATED-1, Boreas, 45, 1–45, https://doi.org/10.1111/bor.12142, 2016.

https://doi.org/10.5194/cp-2023-47
Preprint. Discussion started: 16 June 2023

Hughes, P. D., Gibbard, P. L., and Ehlers, J.: Timing of glaciation during the last glacial cycle: evaluating the concept of a global 'Last Glacial Maximum'(LGM), Earth-Science Reviews, 125, 171–198, https://doi.org/10.1016/j.earscirev.2013.07.003, 2013.

Hulton, N. R., Purves, R., McCulloch, R., Sugden, D. E., and Bentley, M. J.: The last glacial maximum and deglaciation in southern South America, Quaternary Science Reviews, 21, 233–241, https://doi.org/10.1016/S0277-3791(01)00103-2, 2002.

Izumi, K., Valdes, P., Ivanovic, R., and Gregoire, L.: Impacts of the PMIP4 ice sheets on Northern Hemisphere climate during the last glacial period, Climate Dynamics, 60, 2481–2499, https://doi.org/10.1007/s00382-022-06456-1, 2023.

Joussaume, S. and Taylor, K.: Status of the paleoclimate modeling intercomparison project (PMIP), World Meteorological Organization-Publications-WMO TD, pp. 425–430, 1995.

Kageyama, M., Albani, S., Braconnot, P., Harrison, S. P., Hopcroft, P. O., Ivanovic, R. F., Lambert, F., Marti, O., Peltier, W. R., Peterschmitt, J.-Y., et al.: The PMIP4 contribution to CMIP6–Part 4: Scientific objectives and experimental design of the PMIP4-CMIP6 Last Glacial Maximum experiments and PMIP4 sensitivity experiments, Geoscientific Model Development, 10, 4035–4055, https://doi.org/10.5194/gmd-10-4035-2017, 2017.

Kageyama, M., Harrison, S. P., Kapsch, M.-L., Lofverstrom, M., Lora, J. M., Mikolajewicz, U., Sherriff-Tadano, S., Vadsaria, T., Abe-Ouchi, A., Bouttes, N., et al.: The PMIP4 Last Glacial Maximum experiments: preliminary results and comparison with the PMIP3 simulations, Climate of the Past, 17, 1065–1089, https://doi.org/10.5194/cp-17-1065-2021, 2021.

Kohfeld, K. E., Graham, R. M., De Boer, A. M., Sime, L. C., Wolff, E. W., Le Quéré, C., and Bopp, L.: Southern Hemisphere westerly wind changes during the Last Glacial Maximum: paleo-data synthesis, Quaternary Science Reviews, 68, 76–95, https://doi.org/10.1016/j.quascirev.2013.01.017, 2013.

Lambeck, K., Rouby, H., Purcell, A., Sun, Y., and Sambridge, M.: Sea level and global ice volumes from the Last Glacial Maximum to the Holocene, Proceedings of the National Academy of Sciences, 111, 15 296–15 303, https://doi.org/10.1073/pnas.1411762111, 2014.

Liakka, J., Löfverström, M., and Colleoni, F.: The impact of the North American glacial topography on the evolution of the Eurasian ice sheet over the last glacial cycle, Climate of the Past, 12, 1225–1241, https://doi.org/10.5194/cp-12-1225-2016, 2016.

Lofverstrom, M. and Liakka, J.: The influence of atmospheric grid resolution in a climate model-forced ice sheet simulation, The Cryosphere, 12, 1499–1510, https://doi.org/10.5194/tc-12-1499-2018, 2018.

Löfverström, M., Caballero, R., Nilsson, J., and Kleman, J.: Evolution of the large-scale atmospheric circulation in response to changing ice sheets over the last glacial cycle, Climate of the Past, 10, 1453–1471, https://doi.org/10.5194/cp-10-1453-2014, 2014.

Marsiat, I.: Simulation of the Northern Hemisphere continental ice sheets over the last glacial-interglacial cycle: experiments with a latitude-longitude vertically integrated ice sheet model coupled to a zonally averaged climate model, 1994.

Meinshausen, M., Smith, S., Calvin, K., Daniel, J., Kainuma, M., Lamarque, J., Matsumoto, K., Montzka, S., Raper, S., Riahi, K., et al.: The paleoclimate modeling intercomparison project contribution to CMIP5, WCRP Coupled Model Intercomparison Project-Phase 5-CMIP5, 16, 15–51, 2011.

Möller, M. and Schneider, C.: Climate sensitivity and mass-balance evolution of Gran Campo Nevado ice cap, southwest Patagonia, Annals of glaciology, 48, 32–42, https://doi.org/10.3189/172756408784700626, 2008.

Monnin, E., Indermuhle, A., Dallenbach, A., Fluckiger, J., Stauffer, B., Stocker, T. F., Raynaud, D., and Barnola, J.-M.: Atmospheric CO2 concentrations over the last glacial termination, science, 291, 112–114, https://doi.org/10.1126/science.291.5501.112, 2001.

Moreno, P. I., Lowell, T. V., Jacobson Jr, G. L., and Denton, G. H.: Abrupt vegetation and climate changes during the last glacial maximumand last termination in the chilean lake district: a case study from canal de la puntilla (41 s), Geografiska Annaler: Series A, Physical Geography, 81, 285–311, https://doi.org/10.1111/1468-0459.00059, 1999.

https://doi.org/10.5194/cp-2023-47
Preprint. Discussion started: 16 June 2023

Morlighem, M., Williams, C., Rignot, E., An, L., Bamber, J., Chauche, N., Dowdeswell, J., Dorschel, B., Holland, D., Holland, D., et al.: BedMachine v3: Complete bed topography and ocean bathymetry mapping of Greenland from multi-beam radar sounding combined with mass conservation, https://doi.org/10.1002/2017GL074954, 2017.

Morlighem, M., Rignot, E., Binder, T., Blankenship, D., Drews, R., Eagles, G., Eisen, O., Ferraccioli, F., Forsberg, R., Fretwell, P., et al.: Deep glacial troughs and stabilizing ridges unveiled beneath the margins of the Antarctic ice sheet, Nature Geoscience, 13, 132–137, https://doi.org/10.1038/s41561-019-0510-8, 2020.

Parrenin, F., Masson-Delmotte, V., Köhler, P., Raynaud, D., Paillard, D., Schwander, J., Barbante, C., Landais, A., Wegner, A., and Jouzel, J.: Synchronous change of atmospheric CO2 and Antarctic temperature during the last deglacial warming, Science, 339, 1060–1063, https://doi.org/10.1126/science.1226368, 2013.

Patton, H., Hubbard, A., Andreassen, K., Winsborrow, M., and Stroeven, A. P.: The build-up, configuration, and dynamical sensitivity of the Eurasian ice-sheet complex to Late Weichselian climatic and oceanic forcing, Quaternary Science Reviews, 153, 97–121, https://doi.org/10.1016/j.quascirev.2016.10.009, 2016.

Patton, H., Hubbard, A., Andreassen, K., Auriac, A., Whitehouse, P. L., Stroeven, A. P., Shackleton, C., Winsborrow, M., Heyman, J., and Hall, A. M.: Deglaciation of the Eurasian ice sheet complex, Quaternary Science Reviews, 169, 148–172, https://doi.org/10.1016/j.quascirev.2017.05.019, 2017.

Peano, D., Colleoni, F., Quiquet, A., and Masina, S.: Ice flux evolution in fast flowing areas of the Greenland ice sheet over the 20th and 21st centuries, Journal of Glaciology, 63, 499–513, https://doi.org/10.1017/jog.2017.12, 2017.

Peltier, W. R., Argus, D., and Drummond, R.: Space geodesy constrains ice age terminal deglaciation: The global ICE-6G_C (VM5a) model, Journal of Geophysical Research: Solid Earth, 120, 450–487, https://doi.org/10.1002/2014JB011176, 2015.

Rother, H., Fink, D., Shulmeister, J., Mifsud, C., Evans, M., and Pugh, J.: The early rise and late demise of New Zealand's last glacial maximum, Proceedings of the National Academy of Sciences, 111, 11 630–11 635, https://doi.org/10.1073/pnas.1401547111, 2014.

Sato, T. and Greve, R.: Sensitivity experiments for the Antarctic ice sheet with varied sub-ice-shelf melting rates, Annals of Glaciology, 53, 221–228, https://doi.org/10.3189/2012AoG60A042, 2012.

Schneider von Deimling, T., Ganopolski, A., Held, H., and Rahmstorf, S.: How cold was the last glacial maximum?, Geophysical Research Letters, 33, https://doi.org/10.1029/2006GL026484, 2006.

Seroussi, H., Nowicki, S., Payne, A. J., Goelzer, H., Lipscomb, W. H., Abe-Ouchi, A., Agosta, C., Albrecht, T., Asay-Davis, X., Barthel, A., et al.: ISMIP6 Antarctica: a multi-model ensemble of the Antarctic ice sheet evolution over the 21st century, The Cryosphere, 14, 3033–3070, https://doi.org/10.5194/tc-14-3033-2020, 2020.

Shulmeister, J., Thackray, G. D., Rittenour, T. M., Fink, D., and Patton, N. R.: The timing and nature of the last glacial cycle in New Zealand, Quaternary Science Reviews, 206, 1–20, https://doi.org/https://doi.org/10.1016/j.quascirev.2018.12.020, 2019.

Simms, A. R., Lisiecki, L., Gebbie, G., Whitehouse, P. L., and Clark, J. F.: Balancing the last glacial maximum (LGM) sea-level budget, Quaternary Science Reviews, 205, 143–153, https://doi.org/10.1016/j.quascirev.2018.12.018, 2019.

Stokes, C. R.: Deglaciation of the Laurentide Ice Sheet from the Last Glacial Maximum., Cuadernos de investigación geográfica., 43, 377–428, https://doi.org/10.18172/cig.3237, 2017.

Tarasov, L., Dyke, A. S., Neal, R. M., and Peltier, W. R.: A data-calibrated distribution of deglacial chronologies for the North American ice complex from glaciological modeling, Earth and Planetary Science Letters, 315, 30–40, https://doi.org/10.1016/j.epsl.2011.09.010, 2012.

Tierney, J. E., Zhu, J., King, J., Malevich, S. B., Hakim, G. J., and Poulsen, C. J.: Glacial cooling and climate sensitivity revisited, Nature, 584, 569–573, https://doi.org/10.1038/s41586-020-2617-x, 2020.

https://doi.org/10.5194/cp-2023-47
Preprint. Discussion started: 16 June 2023

Troch, M., Bertrand, S., Lange, C. B., Cárdenas, P., Arz, H., Pantoja-Gutiérrez, S., De Pol-Holz, R., and Kilian, R.: Glacial isostatic adjustment near the center of the former Patagonian Ice Sheet (48° S) during the last 16.5 kyr, Quaternary Science Reviews, 277, 107 346, https://doi.org/10.1016/j.quascirev.2021.107346, 2022.

Ullman, D., LeGrande, A., Carlson, A. E., Anslow, F., and Licciardi, J.: Assessing the impact of Laurentide Ice Sheet topography on glacial climate, Climate of the Past, 10, 487–507, https://doi.org/10.5194/cp-10-487-2014, 2014.

Yan, Q., Wei, T., and Zhang, Z.: Modeling the climate sensitivity of Patagonian glaciers and their responses to climatic change during the global last glacial maximum, Quaternary Science Reviews, 288, 107 582, https://doi.org/10.1016/j.quascirev.2022.107582, 2022.

Zech, R., Zech, J., Kull, C., Kubik, P. W., and Veit, H.: Early last glacial maximum in the southern Central Andes reveals northward shift of the westerlies at˜ 39 ka, Climate of the Past, 7, 41–46, https://doi.org/10.5194/cp-7-41-201, 2011.